

**HIGH-QUALITY LGS-TYPE CRYSTALS AND FILMS  
FOR SURFACE ACOUSTIC WAVE APPLICATIONS**

**Final Technical Report**

by Dr. Christine Klemenz  
December 2000

European Research Office of the U.S. Army  
London, England

Contract Number : N68171-99-M-6663, PI : Dr. H. J. Scheel  
R&D 8554-EE-01

Cristallogénèse, Institute of Micro- and Optoelectronics,  
Swiss Federal Institute of Technology Lausanne EPFL.  
SWITZERLAND

**DISTRIBUTION STATEMENT A**  
Approved for Public Release  
Distribution Unlimited

**20010523 039**



Reference number : R&D 8854-EE01  
Contract Number: N68171-99-M-6663, PI. Dr. H. J. Scheel  
Author : Dr. C. Klemenzenz

## **High-quality LGS-type Crystals and Films for Surface Acoustic Wave Applications**

Final technical report, September 1999 - August 2000

### **Abstract**

The aim of this project was to investigate the feasibility of liquid phase epitaxy (LPE) for the growth of high-quality langasite-type films for high-frequency RF resonator applications.

The work done during this period included phase diagram studies, the search for a suitable solvent, systematic flux growth experiments of LGS, LGN and LGT, X-ray analysis of crystallized phases, preparation (orientation, sawing, polishing, etching) of LGS and LGT substrates from provided bulk Czochralski-grown crystals, top-seeded solution growth (TSSG) and LPE experiments.

LPE films of LGS up to  $1 \times 1 \text{ cm}^2$  could be grown on X- and Y-cut (YZ, XZ in-plane axis, respectively) LGS substrates for the first time. The clear tendency to step/facet formation observed on Y-LGS films indicates that this plane (at least) may evolve to the equilibrium facet, e.g. a perfectly oriented and flat surface, which is very interesting in view of SAW & BAW applications.

**Keywords :** Langasite-type crystals, SAW, BAW,  
phase diagrams, flux growth, liquid-phase epitaxy.

### **Table of content**

|       |   |    |
|-------|---|----|
| I.    | Introduction.....   | 2  |
| II.   | Czochralski growth & inhomogeneities in LGS-type materials..... | 4  |
| III.  | Substrates for LPE.....   | 6  |
| IV.   | Phase relations and choice of solvent.....                      | 9  |
| V.    | Flux growth results.....  | 10 |
| VI.   | LPE growth results.....   | 12 |
|       | 6.1. LPE of LGT.....  | 12 |
|       | 6.2. LPE of LGS.....  | 12 |
| VII.  | Conclusions and discussion.....                                 | 16 |
| VIII. | References.....   | 18 |

## I. Introduction

Langasite-type crystals  $\text{La}_3\text{Ga}_5\text{SiO}_{14}$  (LGS),  $\text{La}_3\text{Ga}_5.5\text{Nb}_{0.5}\text{O}_{14}$  (LGN), and  $\text{La}_3\text{Ga}_5.5\text{Ta}_{0.5}\text{O}_{14}$  (LGT) are considered as superior piezoelectric materials for bulk acoustic wave (BAW) and surface acoustic wave (SAW) applications.

LGS, LGN and LGT belong to the same trigonal crystal class 32 than quartz, and can be grown by Czochralski already to relatively large diameters of 3-inch for LGS [1]. However, bulk growth of large LGS-type crystals is faced with several difficulties, and the crystals often present a defect structure (precipitates, inclusions, striations, dislocations, twins, cracks) which may limit their performance in applications.

SAW are very sensitive to the quality of the substrate surface [2,3], and fundamental requirements for reproducibility and precision of SAW devices are defect-free substrate crystals, since it is the only way to have an undisturbed SAW propagation. During SAW propagation, substrate surface displacements are of the order of (typically) few Å, and 90 to 95% of the energy is concentrated within one acoustic wavelength of the surface. It is expected that at higher frequencies, e.g. smaller wavelengths, the contribution of smaller defects (of the order of  $\lambda$ ) will become increasingly important.

Among the defects to be considered, dislocations, low-angle grain boundaries (LAGB), and twins are known to degrade the SAW properties. For defects which imply a reversal of the polar axis, like electrical twins in quartz or residual ferroelectric domains in  $\text{LiNbO}_3$ , the SAW propagation and thus the electrical properties of SAW devices are the strongest affected. Electrical measurements on SAW filters fabricated on twinned substrates show a passband distortion caused by reflection and diffraction on such defects. Inhomogeneous dislocation densities, LAGBs, and different growth sectors in the crystal produce variation of the SAW velocity. Also interaction between various kind of defects has shown to be important. LAGB induce mechanical strains, which set up counterpotentials that cannot be overcome by poling. As consequence, residual ferroelectric domains remains after poling. Furthermore, during the growth of the crystal, existing LAGB multiply, a phenomenon which depends only slightly from the growth parameters and thus cannot be significantly influenced during the growth.

Therefore, only high-quality grain boundary-free seed crystals should be used. In addition, the surface of the seed crystal has to be well prepared and strain-free, since perturbations of the seed surface will also induce GBs in the growing crystal. This applies also to the substrates to be used for liquid-phase epitaxy (LPE), which have to be strain-free and of highest possible quality.

High-temperature solution (or flux) growth is a growth method which has the potential to yield highly perfect crystals (lowest dislocation and defect densities), and films grown by LPE may show a high structural and surface perfection, when growth and substrate parameters are sufficiently met. This has been demonstrated for several materials (ex. : GaAs, GaP, garnets, high- $T_c$  superconductors). Another advantage of near-equilibrium growth is that dopants and impurities will be incorporated in a more homogeneous way than in melt growth. This might be important for reduced acoustic losses for higher  $Q$ , as it was shown for quartz.

In LPE, growth occurs near thermodynamic equilibrium, and it is therefore a technique which is very sensitive to substrate parameters like misfit and misorientation. The availability of LGS, LGN and LGT substrates to be used for LPE (homoepitaxy) represents therefore a serious advantage. In case of homoepitaxy, the supersaturation required to initiate nucleation is extremely small, and inhomogeneities, scratches, as well as residual strain of the polished substrate surface will affect the initial stages of the growth process. Chemical etching is necessary and efficient to remove the damaged surface layer prior to LPE. The substrate misorientation as well as supersaturation should be as small as possible to allow the Frank-van der Merwe (or layer-by-layer) growth mode, for reduced step densities and possibly step bunching [4] (impurities are preferentially trapped at growth steps). A very low supersaturation ( $<<1^\circ\text{C}$ ) is difficult to adjust over the whole substrate surface. Thus, etching and regrowth may occur, which will also depend on substrate surface inhomogeneities, defects, hydrodynamics, and temperature gradients in the solution. When all parameters are well fitted, the LPE surface may evolve to the transition to the facet [5], e.g. the development of an equilibrium crystal facet. Such surface is

perfectly oriented towards defined crystallographic axes, which may cancel problems due to surface misalignment in SAW and BAW devices. However, which surface will develop as equilibrium face depends mainly on the "nature" of the solvent and impurities or additives. Thus, by proper choice of additives, the equilibrium growth habit of crystals can be changed. Finding a suitable solvent/solvent system fulfilling all requirements may therefore represent a real challenge.

## II Czochralski growth & inhomogeneities in LGS-type materials

In LGS-type materials, it was reported [6,7] that the congruent region of crystallization deviate from the stoichiometric composition, and the effect of starting oxides composition on the crystal quality was studied by few groups. In fact, gallium oxide containing melts are well known leading to difficulties in Czochralski growth. The non-stoichiometry, congruency region, and effect of growth atmosphere on melt composition variation and precipitates/inclusions formation were already investigated in the seventeenth, with the development of rare-earth gallium garnets ( $\text{RE}_3\text{Ga}_5\text{O}_{12}$ ;  $\text{RE}=\text{Gd}$  ("GGG"), Nd, Dy, Sm, and solid solutions) as substrates for yttrium and rare-earth iron garnets ( $\text{Y}_3\text{Fe}_5\text{O}_{12}$  "YIG") films for magnetic bubble memory devices [8,9,10]. It was shown that compositional shifts occur due to  $\text{Ga}_2\text{O}_3$  vaporization losses during initial melt down stages and during growth, and a consequence was non-reproducibility, e.g. crystals grown in various laboratories show different compositions and lattice constants [11]. Similar problem is expected for LGS-type materials, with obvious impact on composition- and orientation-dependent piezoelectric properties. In the case of  $\text{RE}_3\text{Ga}_5\text{O}_{12}$  (and  $\text{Y}_3\text{Al}_5\text{O}_{12}$  "YAG"), the effect of melt superheating (heating the melt above the melting temperature) and the time of heating in molten state were related to the crystallization of metastable (perovskite ( $\text{ABO}_3$ ),  $\text{Ga}_2\text{O}_3$  (or  $\text{Al}_2\text{O}_3$ )) phases [12]. In view of this, existing studies (and their conclusions) on LGS materials have to be considered with care. More work on phase relations, stoichiometry/congruency determinations (from sintering and growth experiments) is required. It should be

mentioned that YIG films with the required high quality could only be grown by LPE [13,14]. Neither RF sputtering nor hydrothermal growth could produce the required defect-free films. Vapor-phase epitaxy (VPE) failed due to poor reproducibility and films with high defect densities [13,15].

The major observed inhomogeneities in LGS-type crystals are growth bands or striations, which might be due to the solid-solubility behavior of Si/Ga in LGS, Nb/Ga in LGN and Ta/Ga in LGT, associated with temperature fluctuations at the growth interface. Striations can be made visible by selective etching and optical techniques (see III). Striations cause periodic (3D) variations of lattice parameters, thermal expansion coefficients, and induce local strains. Depending on material and specific growth conditions, the periodicity (as well as 3D pattern within the crystal) of striations can show strong variations. For LGS, periodicities of 35-43 $\mu\text{m}$  [16] and 1-2mm [1] were reported. Striations may be eliminated (or at least reduced) if temperature oscillations at the growth interface can be suppressed. Beside melt composition adjustment, the liquid-solid interface has to be kept as flat as possible during Czochralski growth in order to have the striations within a plane perpendicular to the growth direction.

The striations problem in crystals grown from solutions has been theoretically and experimentally investigated by several authors. The incorporation of an impurity can be expressed in terms of distribution coefficients, and suggested further readings on this topic are [17,18]. In the case of LPE (heteroepitaxy), the distribution coefficients will also depend on the misfit, leading to a dopant incorporation gradient within the thickness of the film. Additionally, when a film is grown by LPE on a striated substrate of same composition (homoepitaxy), one may expect that the first monolayers of the film will try to adapt their composition to minimize the misfit strain (lattice pulling effect). The resulting film will then show a variation of composition in function of its thickness. These combined mechanisms are very complex, differ from one materials group to the other, and need to be investigated from case to case.

### III Substrates for LPE

The importance of the quality of the substrate surface became clear already after the first attempt of LPE of LGS. The surface-layers of polished surfaces have generally residual strain, and chemical etching is required. Polishing and etching of LGS has already been investigated [19,20], and good results were achieved by polishing with colloidal silica and etching with  $\text{HCl}:\text{HF}:\text{H}_2\text{O}$  [19]. It was shown that chemical etching between lapping and polishing is necessary to improve the final substrate surface structure, and various acids,  $\text{HF}$ ,  $\text{HCl}$ ,  $\text{HNO}_3$ ,  $\text{H}_2\text{SO}_4$ ,  $\text{CH}_3\text{COOH}$ , and their mixtures, were tested in these studies. However, the acid which is generally used for perovskite-type compounds (LGO) and garnets is hot orthophosphoric acid.

The provided bulk LGS and LGT crystal pieces were oriented, and substrates cut in the X-, Y-, and Z-orientations (YZ, XZ, XY in-plane axis, respectively). After sawing and lapping with  $\text{SiC}$  and  $\text{Al}_2\text{O}_3$ , the LGS and LGT substrates were etched in hot orthophosphoric acid at  $130^\circ\text{C}$  for 2-3 hours. Formation of the white deposit on the substrate surface could be avoided by mixing. The resulting surface morphology of the Y- and Z-cuts is shown in the Nomarski differential interference contrast microphotographs of figs. 1 a) and b), respectively.

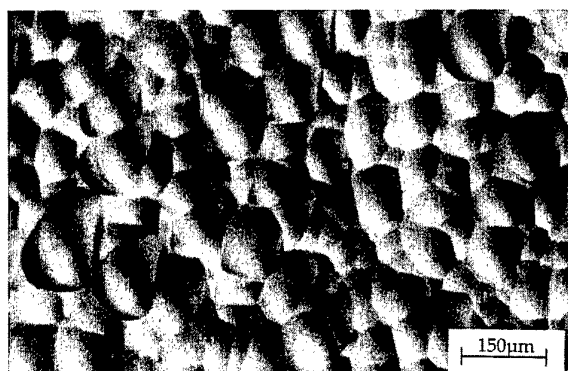
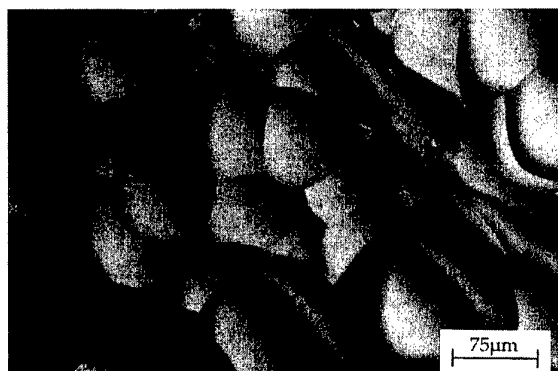


Fig 1. a) Y-cut LGS substrate surface after etching in  $\text{H}_3\text{PO}_4$ .



b) Z-cut LGS surface after same treatment.



Interpretation of Nomarski microphotographs requires careful consideration, since it is often difficult to distinguish between hillocks and hollows. Thus, the structures of fig.1 appear rather as bulging to the eye, whereas in reality they are concave.

Due to the polarity of the X-axis in LGS-type crystals, both X-cut substrate faces are not equivalent, e.g. they have not the same "termination" and behave therefore differently upon etching, see fig.2 a) and b).

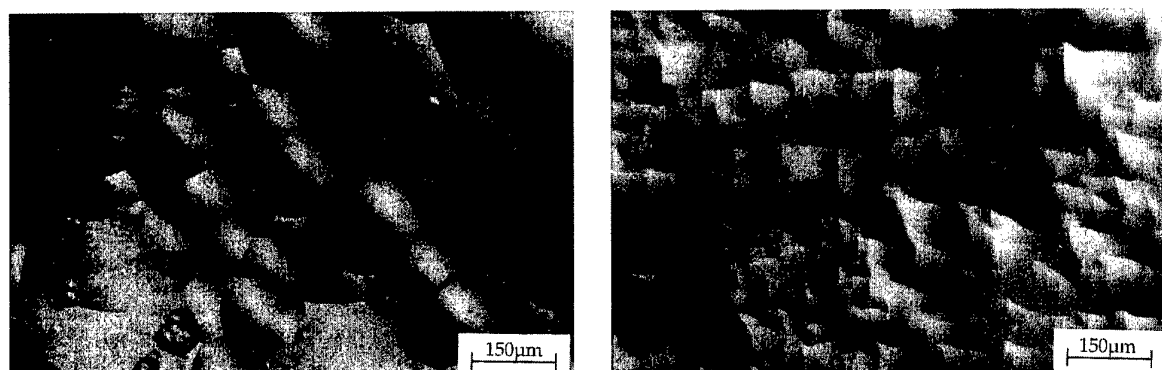


Fig 2. Two sides of the same X-cut LGS substrate after etching in  $\text{H}_3\text{PO}_4$  at  $130^\circ\text{C}$  (3 hours). Due to the polarity, the etch behavior is quite different. Left : A-side, right : B-side.

The LGT substrates show similar patterns, but slightly lower chemical stability in orthophosphoric acid. Randomly oriented crystal faces could not be well etched, which shows certain selectivity of this etchant for major crystal axis. Best results were obtained for the B-side (fig.2, right) of X-cut LGS and LGT. Such etched substrates were mounted with Pt wires on an alumina holder in horizontal position, dipped into the hot  $\text{H}_3\text{PO}_4$ , and rotated at about 300rpm. By this way, striations became visible, as shown in the Nomarski microphotograph of fig 3. On this substrate surface, the growth striae have a depth of about 10nm and a periodicity of about  $5\mu\text{m}$ , and a slight asymmetry can also be noted on the striae profile, which was taken by atomic force microscopy (AFM), fig. 4.

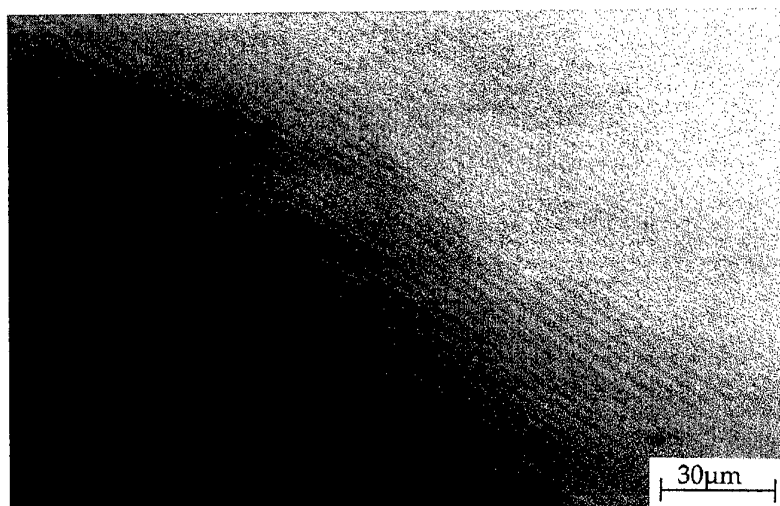


Fig. 3 Nomarski microphotograph of striations on a chemically polished LGT substrate.

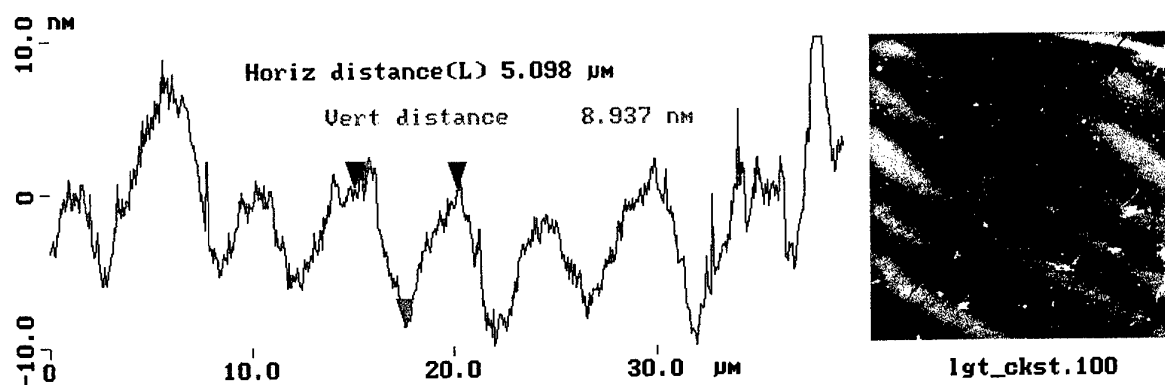


Fig. 4 AFM image and profile of striations on a X-LGT substrate surface revealed after chemical polishing..

For first LPE experiments, when growth conditions and flux composition are not optimized, it is better to use substrates with a rather high step and kink density, since in this case epitaxy may be favored with respect to heterogeneous nucleation under higher supersaturation conditions. However, it is necessary to remove the damaged surface due to sawing and lapping, which will strongly influence nucleation and may lead to crystallization of polycrystalline material rather than an epitaxial film. For these early LPE experiments, LGS substrates with surfaces as shown in figs. 1 & 2 were typically used.

Once the basic growth conditions established, precisely oriented high-quality substrates will be required to further improve the surface perfection of the LPE films.

#### IV Phase relations and choice of solvent

Whereas data on binary compounds can generally be found [21], the phase relations in ternary and in the quaternary systems La-Ga-X-O ( $X=Si, Nb, Ta$ ) are actually not known. A tentative phase diagram has been established by collecting literature data from sintering and crystal growth experiments, and completed by own determinations. This work which is still in progress.

Potential solvent systems for LGS, LGN and LGT were searched through systematic studies of the already available respective or related phase diagrams. First, the efforts were concentrated on LGT and potentially to LGN which shows strong similarities with LGT in the binary phase diagrams. A first selection of possible fluxes was done according to chemical and structural aspects. Ideally, the solvent should be chemically similar (in the type of bonding) to the solute, but with sufficient crystal-chemical differences between solvent and solute constituents to avoid incorporation of solvent species into the crystal. The use of a self-flux is therefore of advantage, but not always possible.

The most common solvent for oxides is PbO. PbO-B<sub>2</sub>O<sub>3</sub> fluxes as well as BaO-BaF<sub>2</sub>-B<sub>2</sub>O<sub>3</sub> ternary solvent systems were successfully used in LPE growth of garnets [22]. PbO-based fluxes were also used for the growth of perovskites ABO<sub>3</sub> ( $A=La, Nd, Pr; B=Ga$ ) [23]. Bi<sub>2</sub>O<sub>3</sub>-based fluxes have similarities with PbO fluxes, and are often used instead of the highly toxic PbO. However, when large RE ions are present, e.g. in LGX, they are not suitable due to possible substitution.

Alkali vanadates, molybdates and tungstates were widely used as fluxes for crystal growth of silicates and germanates. These fluxes were not used for LPE, except one attempt to grow Na<sub>2</sub>CaGe<sub>6</sub>O<sub>14</sub> (langasite structure) LPE films on Nd<sub>3</sub>Ga<sub>5</sub>SiO<sub>14</sub> from K<sub>2</sub>O-V<sub>2</sub>O<sub>5</sub> flux, which was not very successful [24]. Li<sub>2</sub>MoO<sub>4</sub>:MoO<sub>3</sub> dissolves

readily many oxides, and was used for the growth of BeO, GeO<sub>2</sub>, SiO<sub>2</sub>, TiO<sub>2</sub>, Be<sub>2</sub>SiO<sub>4</sub>, Y<sub>2</sub>SiO<sub>5</sub>, as well as for emerald (Be<sub>3</sub>Al<sub>2</sub>Si<sub>6</sub>O<sub>18</sub>). It is known that the morphology of crystals grown from this flux can be modified (from platelets to prisms) by changing the Li<sub>2</sub>MoO<sub>4</sub>:MoO<sub>3</sub> ratio and by additives. If highly perfect LGX platelets could be grown directly from this flux, LPE and subsequent removal of the LPE film from the substrate would not be needed. This was an additional reason to investigate this flux system.

## V Flux growth results

LGT flux experiments with molybdates were done by varying the solute ions concentrations and the Li<sub>2</sub>MoO<sub>4</sub>:MoO<sub>3</sub> ratio (from 1:0 to 1:4). Results obtained with the 1:4 and 1:1 ratios are shown in figs. 5 and 6, respectively.

Interesting observation was that only few La-containing phases were present. This could be tentatively explained by the formation of relatively strong (LaO<sub>x</sub>)<sub>m</sub>(MoO<sub>3</sub>)<sub>u</sub> complexes in the solution. From the La<sub>2</sub>O<sub>3</sub>-MoO<sub>3</sub> phase diagram, further increase of the La<sup>3+</sup> content would have lead to the crystallization of lanthanum molybdates. Therefore, it was preferred to reduce the MoO<sub>3</sub>-content in the flux. The La<sup>3+</sup> concentration was kept at the lowest melting binary eutectic (690°C at approx. 11mol% La<sub>2</sub>O<sub>3</sub>) of the La<sub>2</sub>O<sub>3</sub>-MoO<sub>3</sub> system, and similar approach based on available binary phase relations was used for the other cations. Another interesting observation is that LGO was not formed in the 1:4 flux, whereas β-GaO<sub>2</sub> crystallize from both 1:4 and 1:1 flux ratio. The sequence of complexes stability which can be tentatively deduced is (LaO<sub>x</sub>)<sub>m</sub>(MoO<sub>3</sub>)<sub>u</sub> > (TaO<sub>y</sub>)<sub>n</sub>(MoO<sub>3</sub>)<sub>v</sub> > (GaO<sub>z</sub>)<sub>p</sub>(MoO<sub>3</sub>)<sub>w</sub>, and the temperature dependence is Ga<sub>2</sub>O<sub>3</sub> > LaGaO<sub>3</sub> > LGT > (?). LGT will be formed in the lowest temperature range. This is also consistent with the fact that the lanthanum gallium garnet phase, which would be located between lanthanum gallate and LGT, does not exist [23].

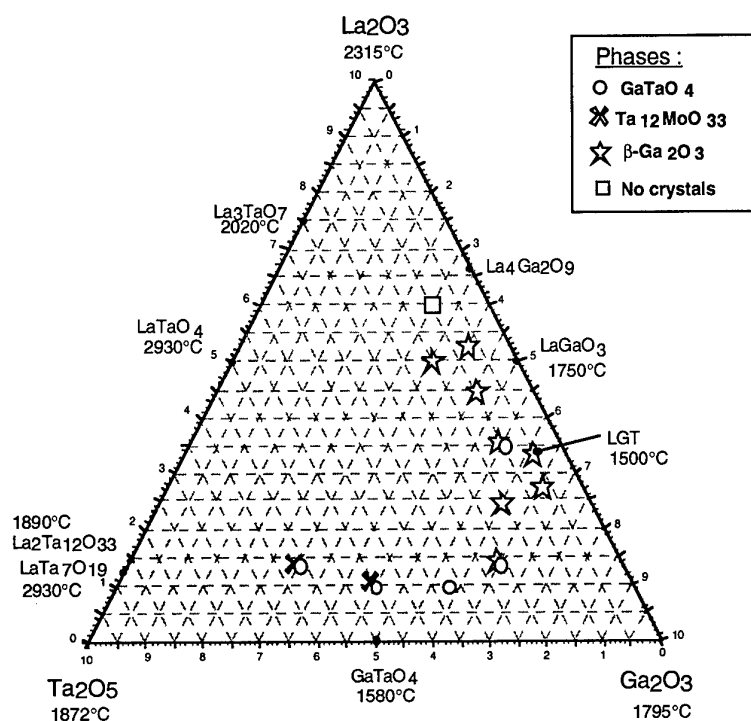


Fig 5. LGT phase relations in the  $\text{Li}_2\text{MoO}_4:\text{MoO}_3$  1:4 flux.

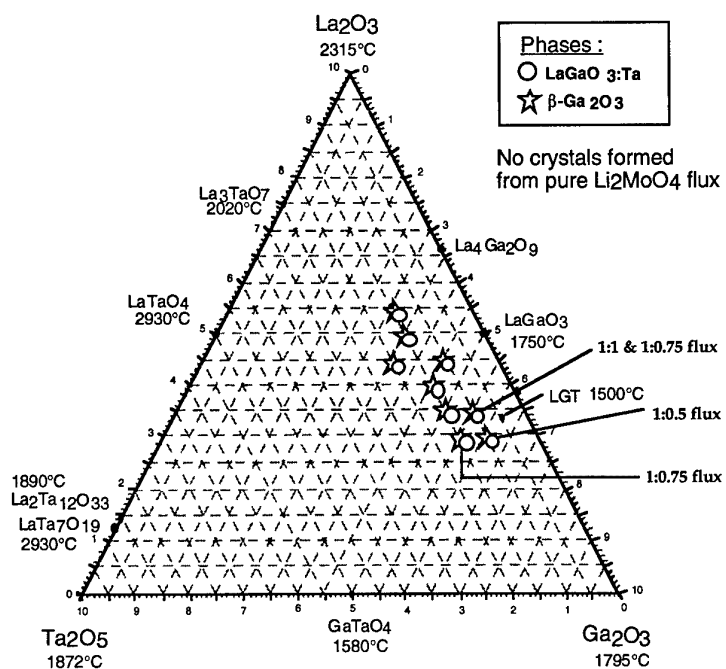


Fig 6. LGT phase relations in the  $\text{Li}_2\text{MoO}_4:\text{MoO}_3$  1:1 flux.

LGS, LGN and LGT growth experiments with a  $\text{PbO-PbO}_2\text{-B}_2\text{O}_3$ -flux yielded  $\text{LaBO}_3$  when  $\text{B}_2\text{O}_3$  was present, as well as  $\text{LaGaO}_3$  (LGO) crystals. Since LGO is expected to crystallize in a higher temperature range than LGX, the soaking temperature and time was lowered in further experiments. Up to now, the LGX phases could not be crystallized from these fluxes in the investigated regions, and this work needs to be continued.

## VI LPE growth results

### 6.1 LPE of LGT

The LPE experiments were performed in a vertical tube furnace equipped with 3 heating zones. With the  $\text{Li}_2\text{MoO}_4\text{:MoO}_3$  flux (1:1-ratio), Ta-doped  $\text{LaGaO}_3$  crystallized on the substrate.  $\text{La,Li(MoO}_4)_2$  was also obtained, depending on respective concentration of solute/solvent species. Strong substrate corrosion occur with this flux, even at solute concentrations up to 50%. Attempts to use a  $\text{PbO}$ -flux yield lead tantalate crystals over a relatively broad concentration/temperature range, and LPE films of LGT could not be grown so far. However, this does not mean that these solvents are not suitable. More work is required to locate the PCF of LGT in the respective phase diagrams and to find additive(s) able to shift chemical equilibria for the crystallization of LGT.

### 6.2 LPE of LGS

For LPE of LGS, a  $\text{PbO}$ -based flux containing typically 15 to 20wt% of solute was used. The starting oxides were well mixed and pressed by hand into a cylindrical Pt/Au crucible. The crucible was closed with a Pt lid to prevent  $\text{PbO}$  evaporation, and placed in the furnace. The temperature was raised to  $800^\circ\text{C}$  in 3 hours, an then to  $1150^\circ\text{C}$  in 4 hours, followed by 5h soaking at this temperature. The temperature was then lowered to above the expected growth temperature, and the Pt lid removed. Search of the liquidus temperature was performed by dipping LGS substrates and crystal pieces in the solution and X-ray analysis of the phases which crystallized on them. This is an efficient

way to locate the crystallization temperature and sequence of the different phases, and can be done within a few days whereas flux growth experiments by slow cooling may require weeks.

LPE films of LGS could be successfully grown in a temperature range of 870 to 950°C, depending on solute content and flux composition. After the growth, the films were cleaned in diluted nitric acid at room temperature, and rinsed with distilled water and then ethanol. Fig. 7 a) and b) are Nomarski microphotographs of a LGS LPE film grown on X-cut LGS substrates, and LGS LPE films grown on Y-cut LGS substrates are shown in figs. 8 a) and b). Fig. 9 is an AFM view and profile of the (macro)step train. On this specific LPE film, large variations of step heights and interstep distances were observed, which is normal for such first films grown under non-optimized substrate, flux, and growth parameters.

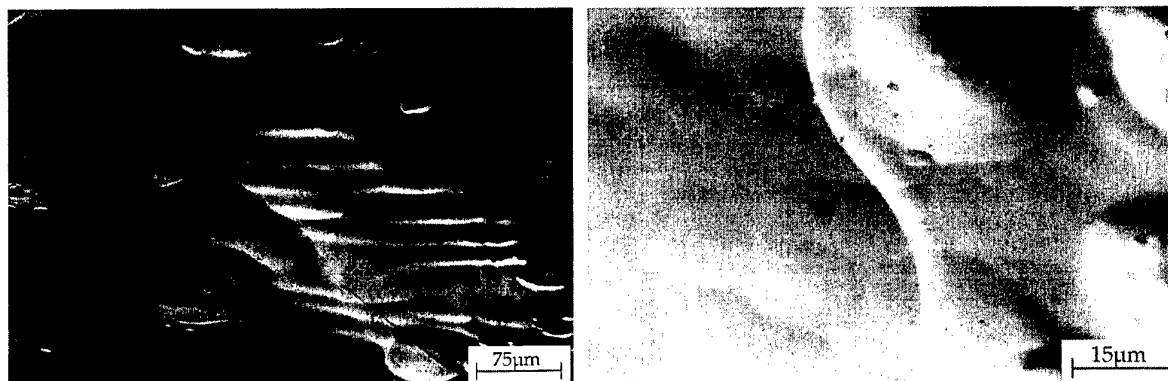


Fig. 7.a) LPE film of LGS on X-cut LGS substrate      b) LPE film of LGS on Y-cut LGS substrate

Whereas the X-oriented films appear more as undulating surfaces with no clear growth habit, the films grown on the Y-cut show a strong tendency to step/facet formation. This is an indication that this surface can develop into an equilibrium face, e.g. transition to faceting is possible at least on the Y-cut.

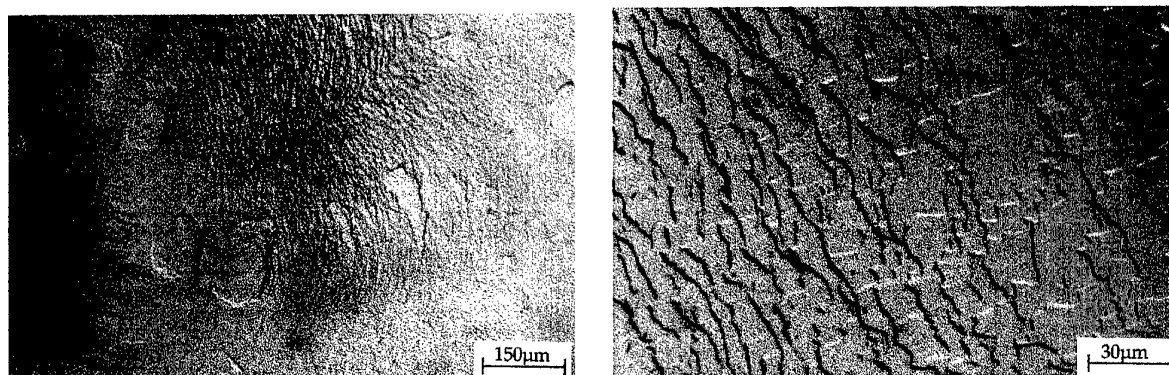


Fig. 8.a) LPE film of LGS on Y-cut LGS substrate. b) Step bunching and macrostep formation.

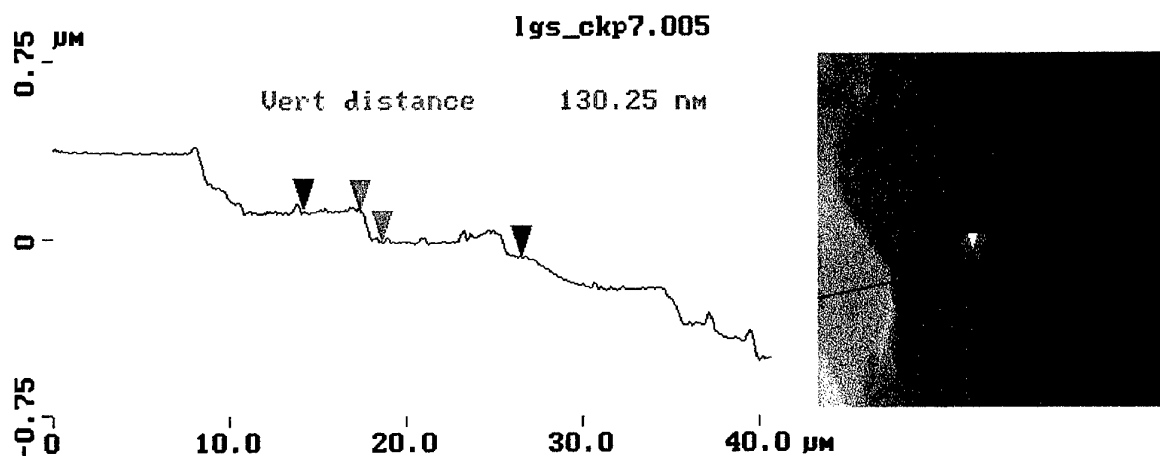


Fig. 9. AFM profile and image of step train on Y-LGS LPE film.

Step bunching can be described by the kinematic wave theory [25], which was developed to explain water flow movements and traffic jam on crowded roads. Step bunches and faceted macrosteps are known to induce striations [26,27,28] and inclusions [26], not only in solution growth of inorganic crystals, but also in the case of organic compounds and biological macromolecules like proteins [29,30].

The mechanisms governing step bunching are not well known, but it is assumed that in solution growth interface kinetics as well as bulk transport are important. Unequal rate of incorporation of growth units in the upper and lower steps, and non-linear dependence of the rate of advance of steps on supersaturation which might be caused by impurities (intermittent pinning or stoppers) belong to possible mechanisms.



In liquid phase epitaxy, substrate misorientation and hydrodynamics are important aspects to be considered to avoid (or reduce) step bunching. Despite its importance, however, there exist no rational way to exclude step bunching, and this problem has to be understood and solved from case to case.

Two of the best Y-oriented LGS LPE films were delivered and analyzed at the U.S. Army Research Laboratory in September 2000. Some of these results are discussed below. The X-ray diffraction analysis show that these films are already of good quality, with a FWHM of  $0.2^\circ$ , which is comparable to the best available Czochralski grown LGS substrates. SEM/EDX analysis allow to image details of the surface structure and that of various defects, and to give a qualitative evaluation of their composition.

In the SEM image of fig. 10, the step train can be reconized (A), as well as needle-like defects (B). The holes (C) are due to the sample preparation processes.



Fig. 10 SEM image of a Y-oriented LGS LPE film surface.

In crystal growth, the following sequence is usually observed with increasing supersaturation/growth instability : near-equilibrium habit – platelets – needles – dendrites/whiskers. On these LPE films, the needle-like defects are an indication of growth instability which may have various origins, for example a higher local supersaturation, hydrodynamics, etc. By adjustment/optimization of all relevant

growth parameters, such defects will be avoided. No secondary phase(s) could be found by XRD and EDX analysis, only a small variation in the composition (qualitative) of needle-like defects with respect to that of the film. In the case of oxides grown from PbO fluxes, Pb incorporation/contamination likely occur, in the form of inclusions or substitution of a lattice ion by Pb. Whereas solvent inclusions can usually be prevented by adjusting the growth rate below a limiting value to avoid instability, substitutions mainly depend on the crystal-chemical aspects of the system, e.g. cannot (usually) be controlled. Often, literature data on Pb-incorporation do not distinguish between the two possibilities, and high reported values are often rather due to solvent inclusions than substitutions. In our LGS films, no Pb-contamination could be found by EDX, e.g. at a detection limit of about 0.1%. Quantitative analysis of the films by secondary ion mass spectroscopy (SIMS) and/or electron microprobe analysis (EMP) is now required in order to determine their stoichiometry and amount of incorporated solvent and additives ions.

Tentatives to measure the thickness of the LGS LPE films by conventional optical/etching methods failed due to the high-quality, strain-free and transparent LPE films, which therefore cannot not be distinguished from the substrate. By SEM, the film thickness could be estimated at about 3-4  $\mu\text{m}$ , see fig. 11, which gives a mean growth rate of about 23  $\text{\AA}/\text{s}$  for this film.

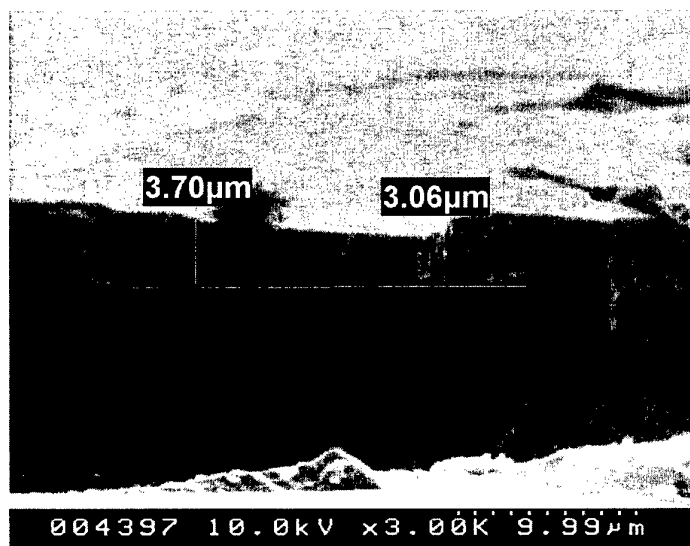


Fig. 11 Measurement of the thickness of a Y-oriented LGS LPE film.

In comparison with LPE of other oxide systems, this growth rate is about 10 times less than the maximum growth rate observed for  $\text{YBa}_2\text{Cu}_3\text{O}_{7-\delta}$  films on  $\text{NdGaO}_3$  [31] and about 5-20 times less the growth rate of magnetic garnet films (depending on rotation velocity) [13,32]. It should also be noted that in LPE of LGS the solution composition/growth parameters are not yet optimized, and values of thickness/growth rate are only valid for the growth conditions/parameters used in these experiments.

## VII Conclusions and discussion

For the first time, LPE films of LGS could be successfully grown on the X- and Y-cut of LGS substrates. The results presented here are recent, with the first LPE films grown in April 2000. Major difficulties arise from the complexity of the system, with huge degrees of freedom of almost all possible solvent/solute variables.

These films show already a very promising surface morphology : step-flow mode on Y-LGS, no cracks, no residual flux, which can be easily removed, and no detected secondary phase(s). Several aspects have to be further investigated : first, the phase formation mechanism of LGS, which is not yet understood. The perovskite phase (LGO) seem to be favored in almost all cases, even in the lower temperature range, and flux growth experiments (without seed) were not successful so far. Possible explanations include a pseudo-metastable behavior due to a concentration range close but not within the primary crystallization field (PCF) of LGS. Etch-back and regrowth is a mechanism which is also frequently observed in LPE, and which possibly occur for these films which were grown close to the thermodynamic equilibrium on relatively rough substrates (see fig.1). However, a dissolving crystal will generally ultimately not be bounded by low index faces, but by curved or rough surfaces, and, on the contrary, the Y-LGS films show a clear faceting over macroscopic dimensions.

Quantitative analysis of the composition of the films (and of the substrates) is now required to understand above mentioned issues and to adjust the flux composition to further improve the quality of the films.

### **Suggestions for further work on this topic are :**

There are three major directions to be considered :

- 1) To continue investigations on LPE of LGS, despite lower piezoelectric performances than LGT (LGN).
- 2) To continue the search for a suitable solvent for LPE of LGT (LGN).
- 3) To investigate ways to obtain a free-standing LPE film of LGX.

#### 1) LPE of LGS :

- systematic LPE experiments with the PbO-based flux.
- quantitative analysis of film (and substrate) composition,
- study/optimization of the flux composition and growth parameters,
- solubility curve determination of LGS in the optimized flux.

To be complemented by : DTA and flux growth to locate the PCF, and theoretical estimation/calculation of the phase diagram,

- electrical measurements to evaluate the effect of deviations from "ideal" LGS composition on piezoelectric properties.

#### 2) LGT and/or LGN

- search for a suitable solvent system (to be continued),
- as above, in case of success.

Major concerns : a) to find a suitable solvent in available time, and b) the effect of stoichiometry changes (solid-solubility behavior between Ga:Ta and Ga:Nb) and other substitutions on piezoelectric properties.

#### 3) Free-standing LPE films

This search has already been started. There exist several possibilities. To grow a LPE film onto a substrate, and to remove the substrate by mechanical means is the less suitable method, due to strain effects. Substrate dissolution with hot  $\text{H}_3\text{PO}_4$  is a better alternative, the LPE film being protected by Pt. Epitaxial lateral overgrowth is also under investigation.

## VIII References

- [1] S. Uda, A. Bungo, C. Jian, *Jpn. J. Appl. Phys.* 38 (1999) 5516.
- [2] H. Matthews, *Surface Wave filters*, Wiley, New York, 1977.
- [3] S. Kelling et al. *J. Chem. Phys.* 107 (1997) 5609.
- [4] C. Klemenz, I. Utke, H.J. Scheel, *J. Crystal Growth* 204 (1999) 62.
- [5] H. J. Scheel, *Appl. Phys. Lett.* 37 (1980) 70.
- [6] H. Takeda, K. Shimamura, V.I. Chani, T. Fukuda, *J. Crystal Growth* 197 (1999) 204.
- [7] M.F. Dubovik, I.A. Andreyev, Yu.S. Shmaly, *IEEE Frequency Control Symposium* (1994) 43.
- [8] R.C. Linares, *J. Crystal Growth* 3,4 (1969) 443.
- [9] C.D. Brandle, D.C. Miller and J. W. Nielsen, *J. Crystal Growth* 12 (1972) 195.
- [10] D. Mateika and Ch. Rusche, *J. Crystal Growth* 42 (1977) 440.
- [11] J.R. Carruthers, M. Kokta, R.L. Barns, M. Grasso, *J. Crystal Growth* 19 (1973) 204.
- [12] M. Göbbels, S. Kimura and T. Sawada, *J. Crystal Growth* 106 (1990) 712.
- [13] M.H. Randles, in : *Crystals : Growth, Properties, and Applications*, Vol.1 : *Crystals for Magnetic Applications*, ed. C.J.M. Rooijmans, Springer, Berlin-Heidelberg-New York, 1978, p. 71-96.
- [14] H.J. Levinstein, S. Licht, R.W. Landorf, S.L. Blank, *Appl. Phys. Lett.* 19 (1971) 486.
- [15] L.J. Varnerin, *IEEE Trans. Magnetics* MAG-7 (1971) 404.
- [16] S.A. Sakharov, Y. Pisarevski, A.V. Medvedev, P.A. Senushencov, V. Lider, *IEEE Frequency Control Symposium* (1995) 642.
- [17] J.A. Burton, R.C. Prim and W.P. Slichter, *J. Chem. Phys.* 21 (1953) 1987.
- [18] D. Elwell and H. J. Scheel, in : *Crystal Growth from High-Temperature Solutions*, Academic Press, London, 1975, reprint by Dover 2000.
- [19] S. Laffey, M. Hendrickson, and J.R. Vig, *IEEE Frequency Control Symposium* (1994) 245.

- [20] A.N. Gotalskaya, D.I. Dresin, S.N. Schegolkova, N.I. Saveleva, V.V. Bezdelkin, G.N. Cherpoukhina, IEEE Frequency Control Symposium (1995) 657.
- [21] Phase diagrams for ceramists, The American Ceramic Society.
- [22] S.L. Blank, in : Crystal Growth : Magnetic Garnets by Liquid Phase Epitaxy, JEMMSE, The Pennsylvania State University, 1979.
- [23] B.E. Watts, H. Dabkowska, and B.M. Wanklyn, J. Crystal Growth 94 (1989) 125
- [24] V.I.Chani, H. Takeda, T. Fukuda, Mat. Sci. & Engng. B60 (1999) 212.
- [25] M.J. Lighthill, G.B. Whitham, Proc. Roy. Soc. 229 (1955) 218 and 317.
- [26] K. Sangwas, R. Rodrigues-Clemente, Surface Morphology of Crystalline Solids, Trans. Tech. Publications, Zurich, 1991)
- [27] E. Bauser, in : Handbook of Crystal Growth, vol. 3C, Ed. D.T.J. Hurle, North-Holland, Amsterdam, 1994.
- [28] T. Nishinaga, K. Pak, S. Uchiyama, J. Crystal Growth 43 (1978) 85.
- [29] F. Rosenberger, P.G. Vekilov, M. Mushol, B. Thomas, J. Crystal Growth 168 (1996) 1.
- [30] A.A. Chernov, J. Crystal Growth 174 (1997) 354.
- [31] C. Klemenz, Liquid-Phase Epitaxy of YBCO and NdBCO High-temperature Superconductors, Ph. D thesis Nr. 14645, The University of Tokyo, March 16, 2000.
- [32] R. Ghez and E.A. Giess, Mat. Res. Bull. 8 (1973) 31.

|   |  |      |  |
|---|--|------|--|
| AD NUMBER   |  | DATE | DTIC ACCESSION<br>NOTICE   |
| 1. REPORT IDENTIFYING INFORMATION   |  |      | <b>REQ:</b><br>1. Put y<br>on re<br>2. Comp<br>3. Attac/<br>malle<br>4. Use u.<br>infor<br>5. Do not<br>for 6 i<br><br><b>DTIC:</b><br>1. Assign<br>2. Return<br><br><b>20010523 039</b> |
| A. ORIGINATING AGENCY<br>SWISS FEDERAL INST. OF TECHNOLOGY, SWITZERLAND   |  |      |  |
| B. REPORT TITLE AND/OR NUMBER<br>HIGH-QUALITY LGS-TYPE CRYSTALS AND FILMS FOR<br>SURFACE ACOUSTIC WAVE APPLICATIONS |  |      |  |
| C. MONITOR REPORT NUMBER<br>R+D 8854-EE-01  |  |      |  |
| D. PREPARED UNDER CONTRACT NUMBER<br>N68171-99-M-6663   |  |      |  |
| 2. DISTRIBUTION STATEMENT<br>APPROVED FOR PUBLIC RELEASE<br>DISTRIBUTION UNLIMITED<br><br>FINAL                     |  |      |  |

OCT 95

S EDITIONS ARE OBSOLETE